Flow of a blood analogue solution through microfabricated hyperbolic contractions

P.C. Sousa, I.S. Pinho
Faculdade de Engenharia da Universidade do Porto, Centro de Estudos de Fenómenos de Transporte, Porto, Portugal.

F.T. Pinho
Faculdade de Engenharia da Universidade do Porto, Centro de Estudos de Fenómenos de Transporte, Departamento de Engenharia Mecânica e Gestão Industrial, Porto, Portugal.

M.S.N. Oliveira, M.A. Alves
Faculdade de Engenharia da Universidade do Porto, Departamento de Engenharia Química, Centro de Estudos de Fenómenos de Transporte, Porto, Portugal.

ABSTRACT: In this work, the flow of a blood analogue solution past a microfabricated hyperbolic contraction followed by an abrupt expansion was studied. The shape of the contraction was selected in order to provide a nearly constant acceleration of the fluid at the centerline of the microgeometry. The flow patterns of the blood analogue solution and of a Newtonian reference fluid were captured using streak line imaging. The flow visualization results illustrate the complex behavior of the blood analogue solution flowing through the microgeometry, which is distinct of that observed for Newtonian fluid flow. For the blood analogue solution, elastic-driven effects are observed with vortical structures emerging upstream of the contraction, which are absent in Newtonian fluid flow. In this latter case the flow also develops inertia-driven instabilities downstream of the expansion. In addition, for the blood analogue solution at high flow rates the competing effects of inertia and elasticity lead to complex flow patterns and unstable flow develops.

1 INTRODUCTION

Human blood is a complex body fluid consisting of a suspension of cellular elements in plasma, 98% of which are erythrocytes (red blood cells, RBCs). Although we can consider plasma as a Newtonian fluid, the deformable RBCs confer non-Newtonian properties to this rheologically complex fluid that exhibits viscoelastic and shear-thinning behavior (Vlastos et al. 1997; Owens 2006). Despite the wealth of information on the complex rheology of blood, a vast majority of research on hemodynamics assumes blood behaves as a Newtonian fluid. This can sometimes be acceptable when blood is flowing through major arteries (Ku 1997). However, non-Newtonian characteristics become important in small vessels or when the characteristic times of the flow and fluid become comparable. Furthermore, viscoelastic effects are enhanced when the vessel geometry exhibits features such as contractions/expansions (e.g. due to fatty deposits), taper or bifurcations in addition to local time dependency.
Since the use of blood in some studies is not always practical, viscoelastic fluids with rheological characteristics similar to human blood are a good alternative. In this work, we compare the flow of a blood analogue solution and the flow of a Newtonian fluid through microfluidic contractions with hyperbolic shape, followed by an abrupt expansion. The micro-contraction has a hyperbolic shape, in order to provide a nearly constant acceleration of the fluid at the centerline of the micro-geometry, as proposed by Oliveira et al. (2007). Using this configuration, it is possible to study the response of the fluid under strong accelerations, for controlled extensional flow conditions (Oliveira et al. 2007).

2 EXPERIMENTAL

2.1 *Microchannel Geometry*

All microchannels used in this study are planar and have a contraction with a hyperbolic shape, followed by an abrupt expansion. In Figure 1 we show a microscopy image of a typical contraction-expansion geometry used in this study.

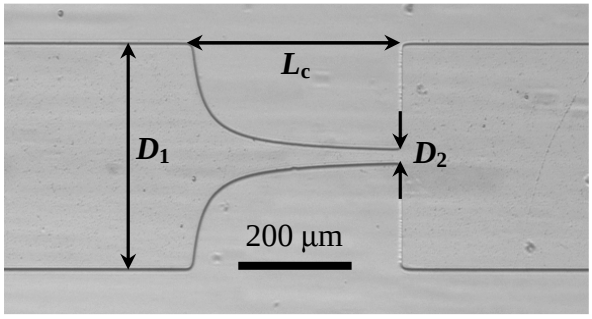

Figure 1. Microchannel used in the experiments (ε_H=3).

The total width, $D_1 = 400$ μm, and the depth, $h = 50$ μm, of the microchannels are kept constant for all geometries. The minimum width of the contraction, D_2, and the hyperbolic contraction length, L_c were varied in order to obtain different values of the total Hencky strain (ε_H), here defined as $\varepsilon_H = \ln(D_1/D_2)$. In Table 1 we present the values used for each geometry.

Table 1. Geometry dimensions.

D_2 (μm)	L_c (μm)	ε_H (-)
147	34.4	1.0
54.1	128	2.0
19.9	382	3.0
10.0	780	3.7

The channels were fabricated in polydimethylsiloxane, PDMS (Sylgard 184, Dow Corning), from an SU-8 photoresist mold using standard soft lithography techniques (McDonald 2000). PDMS was utilized due to its transparency that permits optical access to the flow region, and also due to its simple and well-established fabrication techniques, which allows us to obtain geometries with well-defined features and precise dimensions.

2.2 *Flow Visualization*

Visualizations of the flow patterns were carried out using streak line photography. The optical setup consists of an inverted epi-fluorescence microscope (Leica, DMI5000 M) equipped with a CCD camera (Leica, DFC350 FX), a light source (mercury lamp) and a filter cube (excitation filter BP 530-545 nm, dichroic 565 nm and barrier filter 610-675 nm). A syringe pump (PHD2000, Harvard Apparatus) was used to inject the fluid and control the flow rate in the microchannel. The fluids were seeded with 1 μm fluorescent tracer particles (Nile Red, Molecular Probes, Invitrogen, Ex/Em: 520/580 nm) and sodium dodecyl sulfate (0.1 wt. %, Sigma-Aldrich) was added in order to minimize adhesion of fluorescent particles to the channels walls. The light emitted by the fluorescent particles is imaged through the microscope objective (10×, NA = 0.25) onto the CCD array of the camera using long exposure times (~1 s) in order to capture the particle movement. All of the streakline images presented here are centered at the mid-plane of the microchannel.

2.3 *Rheological Characterization*

The fluids used in the experiments were a xanthan gum aqueous solution (500 ppm w/w), which has a rheological behavior similar to that of human blood (Vlastos et al. 1997) and de-ionized water, which was used for comparison purposes.

The rheology of the xanthan gum (XG) solution was measured under steady shear flow using a shear rheometer (Anton Paar, model Physica MCR301) with a cone-plate geometry (75 mm, 1º angle). Figure 2 compares the measured shear viscosity of the XG solution at 20.0 ºC with reported values for human blood (Turitto 1982). The shear viscosity curve was fitted using a PTT model with a Newtonian solvent contribution. The parameters of the fitted model are: $\varepsilon = 0.05$, $\eta_{solvent} = 0.0015$ Pa·s, $\eta_{polymer} = 0.039$ Pa·s and therefore $\eta_0 = 0.0375$ Pa·s. The relaxation time obtained is $\lambda = 1$ s.

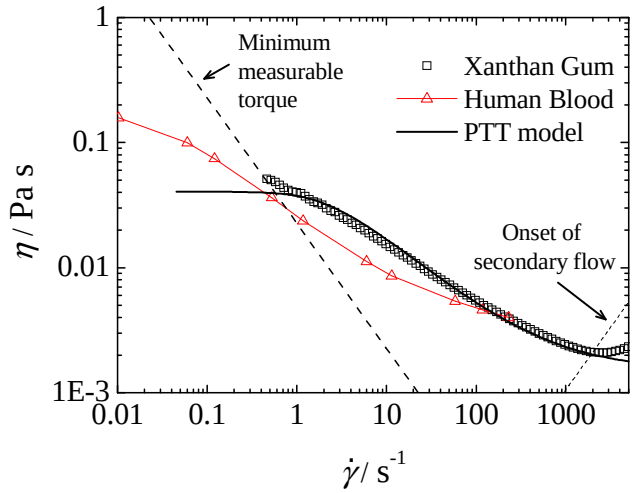

Figure 2. Comparison of steady shear data of the xanthan gum solution at 20.0 ºC with reported values for human blood at 37 ºC (Turitto 1982).

3 RESULTS

3.1 *Newtonian fluid flow patterns*

For comparison purposes, we present the results obtained with a Newtonian fluid (de-ionized water), through the geometries described in Section 2.1.

Figure 3 shows the flow patterns of the Newtonian fluid for a single geometry (ε_H) and varying Reynolds number, defined as:

$$Re = \frac{\rho V_2 D_2}{\eta(\dot{\gamma})} \qquad (1)$$

where ρ is the density of the fluid and V_2 is the average velocity in the region of the contraction with width D_2. For the blood analogue solution the shear-viscosity was estimated at a characteristic shear rate $\dot{\gamma} = V_2/(D_2/2)$. An increase in the flow rate (and therefore in *Re*) leads to the onset of lip vortices close to the re-entrant corner downstream of

the expansion plane. These vortices eventually enlarge to the far corner with increasing *Re*. The value of *Re* at which the onset of lip vortices occurs depends on the geometry used, i.e. for higher Hencky-strain geometries, the onset of lip vortices appears at a lower value of *Re*. Increasing inertia further causes the vortices to grow in size and strength until a critical *Re* is reached. At these critical conditions, the flow becomes asymmetric downstream of the expansion plane, which is in agreement with the findings of Oliveira et al. (2008) using abrupt contractions followed by abrupt expansions. Again the value of the critical *Re* is lower for higher Hencky strain geometries.

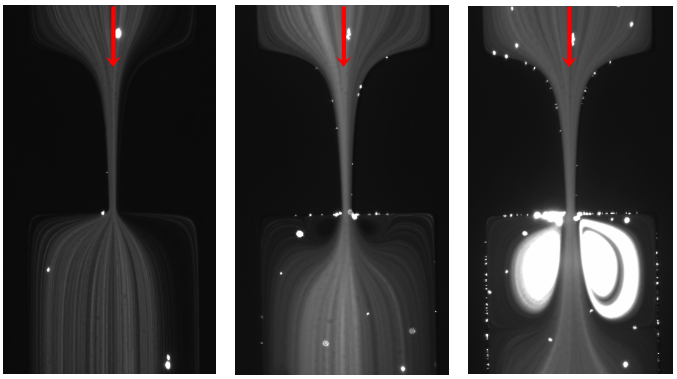

(a) (b) (c)

Figure 3. Streak line images of the Newtonian fluid flow through the microchannels studied with ε_H = 3.0 for (a) *Re* = 5.56, (b) *Re* = 16.7 and (c) *Re* = 44.4.

3.2 *Viscoelastic fluid flow patterns*

In Figures 4 (a) and 4 (b) we show streak line images of the xanthan gum solution flowing through contraction-expansion geometries with $\varepsilon_H = 2$ and $\varepsilon_H = 3$, respectively. The flow patterns observed for the viscoelastic fluid are qualitatively similar for all micro-geometries studied, and only selected images are shown here. The following dimensionless numbers are also used in order to characterize the viscoelastic flow (cf. Figure 1):

$$De_2 = \frac{\lambda(\dot{\gamma})V_2}{D_2/2} \qquad (2)$$

The relaxation time was estimated according to $\lambda(\dot{\gamma}) = N_1/[2\eta(\dot{\gamma})\dot{\gamma}^2]$ and using the fitted PTT model, since the rheometer could not measure N_1 for this fluid.

At very low flow rates, the flow patterns are Newtonian-like, but on increasing the flow rate, symmetric vortices develop upstream of the hyperbolic contraction. Increasing the Deborah number even further leads to an increase of the vortex size due to the enhancement of elastic effects. The formation of vortices close to the far corner upstream of the contraction has also been discussed by McKinley et al. (2007) for flows of a 0.3 wt.% PEO solution in a hyperbolic contraction followed by an abrupt expansion. When the flow rate is increased even further, competing elastic and inertial effects are present and a lip vortex emerges downstream of the expansion plane. As was observed for the Newtonian flow, the lip vortex eventually extends to the far corner with increasing flow rate. Subsequently, inertial effects predominate, leading to a decrease of the vortices located upstream of the hyperbolic contraction and an increase of the vortices located downstream of the expansion plane. At even higher flow rates, the flow becomes unstable with the upstream vortices varying in size asymmetrically.

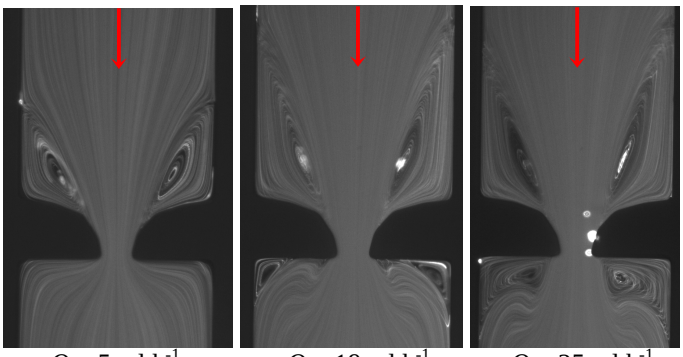

Q = 5 ml h^{-1} *Re* = 17.2 *De* = 57.2 | *Q* = 19 ml h^{-1} *Re* = 68.3 *De* = 91.6 | *Q* = 25 ml h^{-1} *Re* = 90.7 *De* = 101.2

(a)

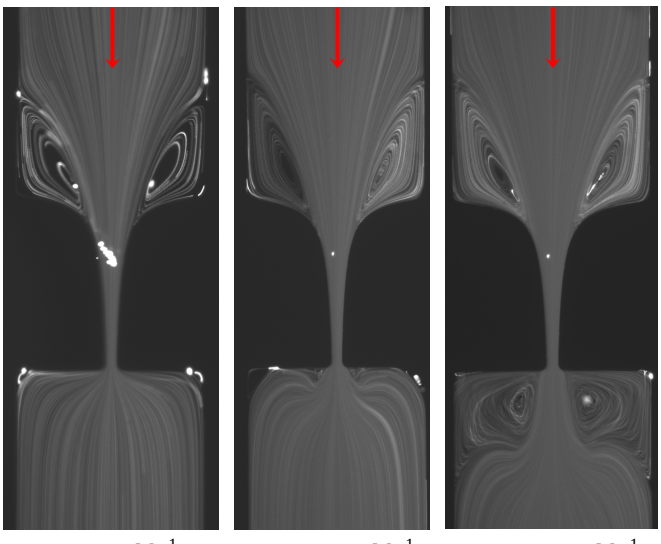

Q = 1 ml h^{-1} *Re* = 3.47 *De* = 55.9 | *Q* = 5 ml h^{-1} *Re* = 18.1 *De* = 98.8 | *Q* = 10 ml h^{-1} *Re* = 36.6 *De* = 128

(b)

Figure 4. Streak line images of xanthan gum solution flowing through a hyperbolic contraction followed by abrupt expansion with (a) ε_H = 2.0 and (b) ε_H = 3.0.

4 CONCLUSIONS

The flow of a viscoelastic blood analogue solution through a microgeometry with a hyperbolic contraction followed by an abrupt expansion exhibits significantly different characteristics from those observed with a Newtonian fluid. In the latter, inertia promotes the appearance of vortices downstream of the abrupt expansion, while in the former complex flow patterns brought about by the elastic nature of the polymeric solution are observed. In this case symmetric vortices appear upstream of the contraction due to elastic effects and when the flow rate is increased, inertial effects lead to a decrease of the upstream vortices and the appearance and growth of downstream vortices. These distinct behaviors clearly show that consideration of blood as a Newtonian fluid is an over-simplification and can prevent a correct prediction of blood flow behavior, especially in small sized vessels.

ACKNOWLEDGEMENTS

The authors gratefully acknowledge funding by FCT via projects PTDC/EQU-FTT/71800/2006, REEQ/262/EME/2005, REEQ/928/EME/2005, and PTDC/EQU-FTT/70727/2006. In addition, PCS and ISP acknowledge the financial support of scholarships SFRH/BD/28846/2006 and CEFT/BII/2008/01.

5 REFERENCES

Ku DN, 1997. Blood flow in arteries. Annual Rev. Fluid Mech., v. 29, pp 399- 434.

Owens J, 2006. A new microstructure-based constitutive model for human blood. Journal of Non-Newtonian Fluid Mech. v. 140, pp. 57–70.

McDonald JC, Duffy DC, Anderson JR, Chiu DT, Wu HK, Schueller OJA, Whitesides GM, 2000. Fabrication of microfluidic systems in poly(dimethylsiloxane). Electrophoresis v. 21, pp. 27–40.

Oliveira, M.S.N., Alves, M.A., Pinho, F.T. and McKinley, G.H., 2007. Viscous flow through microfabricated hyperbolic contractions, Experiments in Fluids, Vol. 43, pp.437-451.

McKinley, G., Rodd, L.E., Oliveira, M.S. and Cooper-White, J., 2007. Extensional flows of polymeric solutions in microfluidic converging/diverging geometries, J. Cent. South Univ. Technol., Vol. 14, pp. 6-9.

Oliveira, M. S. N., Rodd, L. E., McKinley, G. H. and Alves, M. A., 2008. Simulations of extensional flow in microrheometric devices. Microfluidics and Nanofluidics, Vol. 5, pp. 809-826.

Vlastos, G., Lerche, D., Koch, B., Samba, O., Pohl, M., 1997. The effect of parallel combined steady and oscillatory shear flows on blood and polymer solutions. Rheologica Acta, Vol. 36 (2), pp. 160-172.